Journal of Computational Physics **159,** 1–12 (2000)
doi:10.1006/jcph.2000.6445, available online at http://www.idealibrary.com on IDEAL®

Speeding Up Fluid Models for Gas Discharges by Implicit Treatment of the Electron Energy Source Term

G. J. M. Hagelaar* and G. M. W. Kroesen

Eindhoven University of Technology, P.O. Box 513, 5600 MB Eindhoven, The Netherlands
E-mail: *hagelaar@discharge.phys.tue.nl

Received April 22, 1999; revised October 7, 1999

Numerical fluid models are widely used in gas discharge physics. A typical discharge model comprises continuity equations and drift–diffusion equations for reactive particle species, a balance equation for the electron energy, and Poisson's equation for the electric field. When this system of equations is integrated numerically with respect to time, the explicit evaluation of coupled quantities necessitates strong time step restrictions, resulting in an enormous slowdown of the calculation. The strongest time step restriction arises from an explicit treatment of the coupling between the charged particle transport and the space charge field. In order to circumvent this constraint several implicit and semi-implicit techniques have been developed. When one uses these techniques, however, the explicit handling of the dependence of electron energy source term on the electron mean energy becomes limiting for the time step. In this work we present a technique for the implicit treatment of the electron energy source term, based on linearization with respect to the electron mean energy. This approach makes it possible to increase the time step by several orders of magnitude, thus giving a tremendous speedup of the calculation. Test results are provided for some typical cases, covering a wide range of numerical conditions.

Key Words: discharge modeling; plasma modeling; numerical methods; implicit.

INTRODUCTION

Fluid models are widely used in all areas of plasma physics. For gas discharges, various models have been developed in plasma groups all over the world, featuring models for the microdischarges in display panels [1–3], model for RF plasma reactors for deposition or etching [4–6], models for streamer discharges [7–9], and many more. All these models are based on basically the same system of equations, which we will describe now.

0021-9991/00 $35.00

Electron and ion densities are calculated as a function of time and space from the first few moments of the Boltzmann equation. For every species p, a continuity equation reads

$$\frac{\partial n_p}{\partial t} + \nabla \cdot \mathbf{\Gamma}_p = S_p, \tag{1}$$

where n_p is the density, $\mathbf{\Gamma}_p$ is the flux, and S_p is the source term. The flux is given by the second moment of the Boltzmann equation, which is usually approximated by the drift–diffusion equation

$$\mathbf{\Gamma}_p = \mathrm{sgn}(q_p)\mu_p \mathbf{E} n_p - D_p \nabla n_p. \tag{2}$$

$\mathbf{E}$ is the electric field, q_p is the particle charge, μ_p is the mobility, and D_p is the diffusion coefficient. The first term on the right-hand side gives the flux due to the electric field (drift) and the second term represents the flux due to concentration gradients (diffusion). The electric field is dependent on the space charge density according to Poisson's equation

$$\nabla \cdot (\varepsilon \mathbf{E}) = \rho, \tag{3}$$

where ε is the dielectric permittivity and ρ is the space charge density:

$$\rho = \sum_p q_p n_p. \tag{4}$$

The particle source term S_p results from the reactions occurring in the plasma. It consists of positive contributions of the reactions in which a particle of species p is created and of negative contributions of the reactions in which such a particle is lost:

$$S_p = \sum_r N_{p,r} R_r. \tag{5}$$

The index r refers to a reaction. $N_{p,r}$ is the net number of particles of species p created in one reaction of type r, and it can be negative or positive. The reaction rate R_r is proportional to the densities of the reacting particles,

$$R_r = k_r n_{1,r} n_{2,r} \tag{6}$$

for two-body reactions and

$$R_r = k_r n_{1,r} n_{2,r} n_{3,r} \tag{7}$$

for three-body reactions. The proportionality constant k_r is called the reaction rate coefficient.

The transport equations (1)–(2) require the input of the transport coefficients μ and D and the reaction rate coefficients k. In general these quantities depend on the energy distribution of the considered particles. Several approximations have been done concerning these dependencies. Early works [10, 11] used a local field approximation, which assumes a direct relation between the particle energy distributions and the electric field. Transport and rate coefficients are regarded as functions of the electric field:

$$\mu = \mu(E), \qquad D = D(E), \qquad k = k(E). \tag{8}$$

These relations can be found in the literature as results of classical theories and experimental measurements. In many types of discharges, however, the local field approximation is not justified for electrons, so that the use of relations (8) for coefficients concerning electrons leads to unsatisfactory modeling results. More recent works [2, 4–6, 12] therefore assume the electron transport coefficients and the rate coefficients of electron impact reactions to be functions of the electron mean energy

$$\mu_e = \mu_e(\bar{\varepsilon}), \qquad D_e = D_e(\bar{\varepsilon}), \qquad k = k(\bar{\varepsilon}), \tag{9}$$

where the subscript e refers to electrons and the electron mean energy $\bar{\varepsilon}$ is calculated as a function of time and space from an energy balance equation,

$$\frac{\partial n_\varepsilon}{\partial t} + \nabla \cdot \mathbf{\Gamma}_\varepsilon = S_\varepsilon, \tag{10}$$

where n_ε is the electron energy density,

$$n_\varepsilon = n_e \bar{\varepsilon}, \tag{11}$$

and $\mathbf{\Gamma}_\varepsilon$ is the electron energy flux,

$$\mathbf{\Gamma}_\varepsilon = -\frac{5}{3}\mu_e \mathbf{E} n_\varepsilon - \frac{5}{3} D_e \nabla n_\varepsilon. \tag{12}$$

The electron energy source term S_ε is given by

$$S_\varepsilon = -e\mathbf{\Gamma}_e \cdot \mathbf{E} - n_e \sum_r \varepsilon_r k_r n_r. \tag{13}$$

The two terms on the right-hand side represent the heating by the electric field and the energy loss in collisions, respectively. The summation in the collisional loss term is only over the electron impact reactions, with n_r the density of the target particles and ε_r the threshold energy. The functions (9) are calculated from cross sections, with additional assumptions made for the electron energy distribution function. The electron diffusion coefficient is usually found from the electron mobility by the Einstein relation:

$$D_e = \frac{2\mu_e \bar{\varepsilon}}{3e}. \tag{14}$$

The transport equations (1)–(2) for heavy particles are usually solved for the boundary condition of zero particle influx. The boundary conditions for the transport of electrons (1)–(2) and electron energy (10)–(13) include influx by secondary electron emission.

SOLUTION OF THE SYSTEM OF EQUATIONS

When solving this system of equations numerically, one has to deal with the couplings between the different equations. We will demonstrate now how this is usually taken care of in the discretization scheme for time integration. The words “explicit” and “implicit” will turn out to be the key words in resolving the couplings in the system.

Let superscripts refer to a moment in time, and let Δt be a time step, with $t^{k+1} = t^k + \Delta t$. Assume that the values of all quantities are known at a time t^k and are to be calculated at time t^{k+1}. The continuity equations for particles (1) and for electron energy (10) are discretized in time as

$$\frac{n_p^{k+1} - n_p^k}{\Delta t} - \nabla \cdot \mathbf{\Gamma}_p^l = S_p^m, \tag{15}$$

where l and m are the time indices pertinent to Γ and S, respectively. The transport term and the source term can be evaluated either at time t^k ($l = m = k$) or at time t^{k+1} ($l = m = k+1$). Evaluation at time t^k is explicit, since all quantities at t^k are already known. This is computationally attractive, but it can lead to fluctuations or even instabilities in the calculation, unless restrictions are applied to the time step Δt. Evaluation at time t^{k+1} must be implicit, since no values are known yet. Implicit treatment does not lead to fluctuations or instabilities, but it can be very hard to accomplish. Couplings between different equations and nonlinearities can make implicit evaluations quite cumbersome or impossible. We now write Eq. (15) more precisely,

$$\frac{n_p^{k+1} - n_p^k}{\Delta t} - \nabla \cdot \mathbf{\Gamma}_p\left(n_p^{l_n}, \mathbf{E}^{l_\mathbf{E}}, \mu_p^{l_\mu}, D_p^{l_D}\right) = S_p\left(n_1^{m_n}, n_2^{m_n}, \ldots, k_1^{m_k}, k_2^{m_k}, \ldots\right), \tag{16}$$

and discuss in detail the treatment of the different quantities appearing in the transport and source terms of this equation:

- The density in the transport term is always handled implicitly, $l_n = k+1$, because explicit treatment ($l_n = k$) would lead to very severe time step restrictions due to a fundamental necessary condition for the convergence of difference methods, known as the CFL condition [13, 14].
- The evaluation of the electric field in the transport term has drawn the attention of many authors in the field for discharge modeling. If the electric field in the transport term is treated explicitly ($l_\mathbf{E} = k$), as is done in conventional discharge models, the time step condition [10]

$$\Delta t < \frac{\varepsilon_0}{\sum_p |q_r| \mu_p n_p} \tag{17}$$

must be applied in order to avoid numerical instabilities. The electric field at t^{k+1} can then be calculated straightforwardly after the calculation of the densities:

$$\nabla \cdot (\varepsilon \mathbf{E}^{k+1}) = \sum_p q_p n_p^{k+1}. \tag{18}$$

The constraint (17) can be very prohibitive, especially for high plasma densities ($>10^9$ cm^{-3}). Implicit evaluation of $\mathbf{E}$ ($l_\mathbf{E} = k+1$) circumvents this time step restriction, but is numerically unattractive, since it implies solving all the continuity equations (1) and Poisson's equation (3) at the same time. In 1-D models fully implicit techniques have been successfully applied [15, 16], but for multidimensional problems these become too cumbersome. However, it can be shown that, in order to avoid restriction (17), a strictly implicit evaluation of $\mathbf{E}$ is not necessary: a so-called semi-implicit treatment [17–19] will also ensure

stability. In this case, Poisson's equation is solved before the continuity equations. Since the space charge density at time t^{k+1} is not known yet, an estimate is used,

$$\nabla \cdot (\varepsilon \mathbf{E}^{k+1}) = \sum_p q_p \tilde{n}_p^{k+1}, \tag{19}$$

where $\tilde{n}_p^{k+1}$ is an estimate for n_p^{k+1}, arising from the continuity equation (16) with $l_n = l_\mu = l_D = m_n = m_k = k$ and only $l_\mathbf{E} = k+1$:

$$\tilde{n}_p^{k+1} = n_p^k + \Delta t \nabla \cdot \mathbf{\Gamma}_p\left(n_p^k, \mathbf{E}^{k+1}, \mu_p^k, D_p^k\right). \tag{20}$$

Note that the source term S_p has been omitted, since it does not create any space charge: after substitution in Eq. (19), all source terms would cancel. With this semi-implicit technique, the time step can be several orders of magnitude larger than the time step given by constraint (17), thus giving a tremendous speedup of the calculation.

- Transport coefficients and particle source terms are usually evaluated explicitly ($l_\mu = l_D = m_n = m_k = k$). Fully implicit treatment of all densities in the particle source term ($m_n = k+1$) is hardly feasible. Furthermore, implicit evaluation of transport and rate coefficients ($l_\mu = l_D = m_k = k+1$) is problematic since they are arbitrary functions of the electric field (8) or the electron mean energy (9), usually read from lookup tables.

IMPLICIT TREATMENT OF THE ELECTRON ENERGY SOURCE TERM

Using a (semi-)implicit treatment of the electric field in the drift–diffusion flux, we can solve particle transport equations reasonably well. However, it turns out that the solution of the electron energy balance equation becomes limiting for the time step. Small oscillations in the solution of this equation are amplified and spread rapidly throughout the whole system of equations due to the strong dependence of rate coefficients and electron diffusion coefficient on the electron mean energy. A typical behavior is depicted in Fig. 1. It has

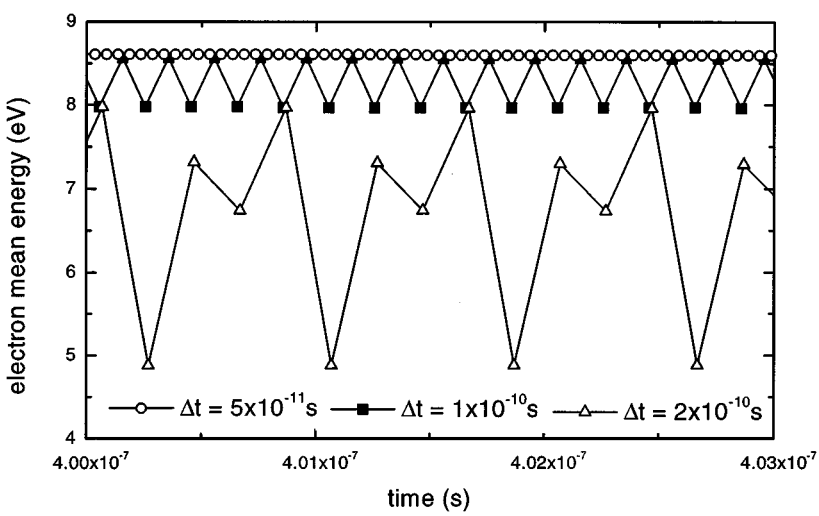

FIG. 1. Oscillations in the electron mean energy at one position in a simulation of a DC microdischarge, for different values of the time step Δt.

been stated previously that this problem can be avoided by evaluating the source term for electron energy implicitly, rather than applying the conventional explicit treatment. For example, Ref. [19] reports a semi-implicit treatment of the inelastic energy losses, albeit for a different type of energy equation. In this work we present an implicit technique for the entire source term (13) of the electron energy equation (10), that is, including the electron heating term.

The electron energy source term has a form different from that of the particle source terms:

$$S_\varepsilon = -e\mathbf{E}^{m_\mathbf{E}} \cdot \mathbf{\Gamma}_e\left(n_e^{m_n}, \mathbf{E}^{m_\mathbf{E}}, \mu_e^{m_\mu}, D_e^{m_D}\right) - n_e^{m_n} \sum_r \varepsilon_r k_r^{m_k} n_r^{m_n}. \tag{21}$$

In this source term the electric field and the electron density can be taken at time t^k without any problem ($m_\mathbf{E} = m_n = k$), but an explicit evaluation of the electron mobility, electron diffusion coefficient, and especially the reaction rate coefficients ($m_\varepsilon = m_\mu = m_D = m_k = k$) can easily cause and amplify fluctuations. We will show now how these quantities can be evaluated implicitly ($m_\varepsilon = m_\mu = m_D = m_k = k+1$). First, we linearize the energy source term with respect to the electron mobility, electron diffusion coefficient, and rate constants:

$$\begin{aligned} S_\varepsilon = &-e\mathbf{E}^k \cdot \mathbf{\Gamma}_e^k - n_e^k \sum_r \varepsilon_r k_r^k n_r^k - e\mathbf{E}^k \cdot \left(\frac{\partial \mathbf{\Gamma}_e}{\partial \mu_e}\right)^k \left(\mu_e^{k+1} - \mu_e^k\right) \\ &- e\mathbf{E}^k \cdot \left(\frac{\partial \mathbf{\Gamma}_e}{\partial D_e}\right)^k \left(D_e^{k+1} - D_e^k\right) - n_e^k \sum_r \varepsilon_r \left(k_r^{k+1} - k_r^k\right) n_r^k. \end{aligned} \tag{22}$$

Then, we linearize the dependencies of these quantities on the electron mean energy,

$$\mu_e^{k+1} = \mu_e^k + \left(\frac{\partial \mu_e}{\partial \bar{\varepsilon}}\right)^k \left(\bar{\varepsilon}^{k+1} - \bar{\varepsilon}^k\right), \tag{23}$$

and analogous expressions for D_e^{k+1} and k_r^{k+1}. Finally, we use

$$\begin{aligned} \bar{\varepsilon}^{k+1} &= \bar{\varepsilon}^k + \left(\frac{\partial \bar{\varepsilon}}{\partial n_\varepsilon}\right)^k \left(n_\varepsilon^{k+1} - n_\varepsilon^k\right) + \left(\frac{\partial \bar{\varepsilon}}{\partial n_e}\right)^k \left(n_e^{k+1} - n_e^k\right) \\ &= \bar{\varepsilon}^k + \frac{1}{n_e^k}\left(n_\varepsilon^{k+1} - n_\varepsilon^k\right) - \frac{n_\varepsilon^k}{\left(n_e^k\right)^2}\left(n_e^{k+1} - n_e^k\right) \\ &= \bar{\varepsilon}^k + \frac{1}{n_e^k}\left(n_\varepsilon^{k+1} - n_e^{k+1}\bar{\varepsilon}^k\right). \end{aligned} \tag{24}$$

Substitution of these expressions into Eq. (22) yields

$$\begin{aligned} S_\varepsilon = &-e\mathbf{E}^k \cdot \mathbf{\Gamma}_e^k - n_e^k \sum_r \varepsilon_r k_r^k n_r^k - \left[\frac{e}{n_e^k}\mathbf{E}^k \cdot \left(\frac{\partial \mathbf{\Gamma}_e}{\partial \mu_e}\right)^k \left(\frac{\partial \mu_e}{\partial \bar{\varepsilon}}\right)^k \right. \\ &\left. + \frac{e}{n_e^k}\mathbf{E}^k \cdot \left(\frac{\partial \mathbf{\Gamma}_e}{\partial D_e}\right)^k \left(\frac{\partial D_e}{\partial \bar{\varepsilon}}\right)^k + \sum_r \varepsilon_r \left(\frac{\partial k_r}{\partial \bar{\varepsilon}}\right)^k n_r^k\right] \left(n_\varepsilon^{k+1} - n_e^{k+1}\bar{\varepsilon}^k\right). \end{aligned} \tag{25}$$

The last term on the right provides an implicit correction of the energy source term for changes in the electron mean energy, which prevents oscillations in the solution of the energy equation. Possible time step restrictions arising from the truncation errors in the

linearizations (22)–(24) are usually not severe, since the transport and rate coefficients are smooth functions of the electron mean energy. Notice that it is essential for this approach that the continuity equation for electrons be solved before solving the energy equation, so that n_e^{k+1} is known.

Combining this technique with the semi-implicit treatment of the electric field discussed in the previous section, we end up with the following scheme:

- First $\mathbf{E}^{k+1}$ is solved from

$$\nabla \cdot (\varepsilon \mathbf{E})^{k+1} = \sum_p q_p \left(n_p^k + \Delta t \nabla \cdot \mathbf{\Gamma}_p \left(n_p^k, \mathbf{E}^{k+1}, \mu_p^k, D_p^k \right) \right). \tag{26}$$

- Then for every species p the density n_p^{k+1} is solved from

$$\frac{n_p^{k+1} - n_p^k}{\Delta t} - \nabla \cdot \mathbf{\Gamma}_p \left(n_p^{k+1}, \mathbf{E}^{k+1}, \mu_p^k, D_p^k \right) = S_p^k. \tag{27}$$

- Finally, n_ε^{k+1} is calculated from

$$\begin{aligned} &\frac{n_\varepsilon^{k+1} - n_\varepsilon^k}{\Delta t} - \nabla \cdot \mathbf{\Gamma}_\varepsilon \left(n_\varepsilon^{k+1}, \mathbf{E}^{k+1}, \mu_e^k, D_e^k \right) \\ &= S_\varepsilon^k - \left[\frac{e}{n_e} \mathbf{E} \cdot \left(\frac{\partial \mathbf{\Gamma}_e}{\partial \mu_e} \frac{\partial \mu_e}{\partial \bar{\varepsilon}} + \frac{\partial \mathbf{\Gamma}_e}{\partial D_e} \frac{\partial D_e}{\partial \bar{\varepsilon}} \right) + \sum_r \varepsilon_r \left(\frac{\partial k_r}{\partial \bar{\varepsilon}} \right) n_r \right]^k \left(n_\varepsilon^{k+1} - n_e^{k+1} \bar{\varepsilon}^k \right). \end{aligned} \tag{28}$$

SPATIAL DISCRETIZATION

The numerical solution of Eqs. (26)–(28) requires an appropriate spatial discretization. In order to ensure a proper functioning of the semi-implicit method for the electric field and the implicit correction of the electron energy source term, the spatial discretization schemes for the different equations (26)–(28) must be consistent with one another. The crucial quantity is the drift–diffusion flux: in each of the equations it should be discretized likewise. We will show how this is done for problems in one spatial dimension. Let subscripts refer to a position in space, and let Δx be a spatial interval, with $x_{i+1} = x_i + \Delta x$.

The drift–diffusion flux in the transport term of the continuity equations (27) and (28) is usually [4–6, 11, 16] discretized according to the exponential scheme of Sharfetter and Gummel [20]. This scheme supports large density gradients, as opposed to the more straightforward central difference scheme. It is based on the analytical solution for a constant drift–diffusion flux between two grid points. In one spatial dimension it reads

$$\Gamma_{i+1/2} = -\frac{1}{\Delta x} D_{i+1/2} \left(f_1(z_{i+1/2}) n_{i+1} - f_2(z_{i+1/2}) n_i \right), \tag{29}$$

where $z_{i+1/2}$ is given by

$$z_{i+1/2} = \frac{\operatorname{sgn}(q) \mu_{i+1/2} E_{i+1/2} \Delta x}{D_{i+1/2}}, \tag{30}$$

and the functions $f_1(z)$ and $f_2(z)$ are defined as

$$f_1(z) = \frac{z}{\exp(z) - 1}, \tag{31}$$

$$f_2(z) = \frac{z \exp(z)}{\exp(z) - 1}. \tag{32}$$

The exponential scheme (29) should now also be applied to the fluxes in the semi-implicit version of Poisson's equation and in the implicit correction of the electron heating.

For the fluxes in Poisson's equation (26), however, this scheme is not very convenient, because it has the electric field appearing within exponential functions, which makes it hard to solve for it. This problem is usually straightforwardly circumvented by using the central difference scheme in this case, which is linear in the electric field:

$$\Gamma_{i+1/2} = \left[\mathrm{sgn}(q)\mu_{i+1/2}\frac{1}{2}(n_{i+1}+n_i)\right]^k E_{i+1/2}^{k+1} - \left[D_{i+1/2}\frac{n_{i+1}-n_i}{\Delta x}\right]^k. \tag{33}$$

However, we found it to be more numerically consistent to stick to the exponential scheme and linearize this in t^k,

$$\begin{aligned}\Gamma_{i+1/2} = {} & [\mathrm{sgn}(q)\mu_{i+1/2}(g_1(z_{i+1/2})n_{i+1} - g_2(z_{i+1/2})n_i)]^k E_{i+1/2}^{k+1} \\ & - \left[D_{i+1/2}h(z_{i+1/2})\frac{n_{i+1}-n_i}{\Delta x}\right]^k,\end{aligned} \tag{34}$$

where the functions $g_1(z)$, $g_2(z)$, and $h(z)$ are defined as

$$g_1(z) = \frac{\partial f_1(z)}{\partial z} = \frac{(1-z)\exp(z)-1}{(\exp(z)-1)^2}, \tag{35}$$

$$g_2(z) = \frac{\partial f_2(z)}{\partial z} = \exp(z)\frac{\exp(z)-(1+z)}{(\exp(z)-1)^2}, \tag{36}$$

$$h(z) = f_1(z) - g_1(z)z = f_2(z) - g_2(z)z = \frac{z^2\exp(z)}{(\exp(z)-1)^2}. \tag{37}$$

The use of expression (34) for the fluxes in the semi-implicit Poisson equation gives better results than the central difference scheme (33), as will be shown in the next section.

Applying the exponential scheme to the electron flux in the electron energy source term and using the Einstein relation (14) yields the following expression for the implicit electron heating correction,

$$\begin{aligned}\left(\frac{\partial\Gamma_e}{\partial\mu_e}\frac{\partial\mu_e}{\partial\bar{\varepsilon}} + \frac{\partial\Gamma_e}{\partial D_e}\frac{\partial D_e}{\partial\bar{\varepsilon}}\right)_{i+1/2} = {} & -\frac{2}{3e\Delta x}\mu_{e,i+1/2}h(z_{i+1/2})(n_{e,i+1}-n_{e,i}) \\ & + \frac{1}{\mu_{e,i+1/2}}\left(\frac{\partial\mu_e}{\partial\bar{\varepsilon}}\right)_{i+1/2}\Gamma_{e,i+1/2,j},\end{aligned} \tag{38}$$

which contains once again the function $h(z)$ given by (37).

TESTING THE IMPLICIT SCHEME

The time integration scheme (26)–(28), which combines the semi-implicit technique for the electric field and the implicit treatment of the electron energy source term, has been extensively tested in 2-D simulations of the microdischarges used in plasma-addressed liquid crystal display panels. In this section we will discuss some typical cases. Figure 2 shows a typical microdischarge geometry, this configuration was used for the test calculations discussed here.

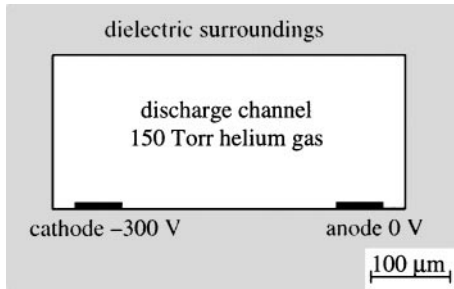

FIG. 2. Two-dimensional microdischarge geometry used in test calculations.

First we considered the simulation of the ignition of a DC discharge, which is one of the most transient phenomena in glow discharges. In this case the behavior of the plasma is governed by ionization processes and the development of extremely high space charge fields. Under these conditions an explicit evaluation of the electron energy source term turned out to result in strong fluctuations in the electron mean energy for $\Delta t > 10^{-10}$ s. Applying the implicit treatment to the electron energy source term made it possible to use time steps up to $\Delta t = 10^{-8}$ s, without any significant influence on the calculation results. For larger time step values, errors in the calculation results could be observed, although even then the calculation remained stable. All calculations yielded exactly the same steady state results, regardless of time step or integration method. Using the implicit method only slightly increased the computational effort per iteration, so that the speedup gained by the increased time step was tremendous. These calculations are represented in Fig. 3, which shows the calculated development of the space averaged electron density for different time steps. Figure 4 shows similar curves for the simulation of the afterglow, i.e., the decay of the plasma after the DC voltage over the electrodes has been switched off. The plasma conditions are completely different now: the electric fields and the electron mean energy decrease rapidly, and the

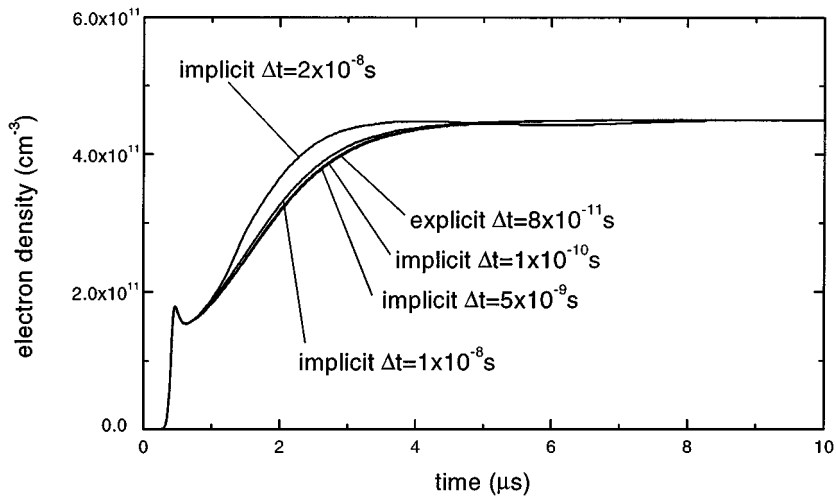

FIG. 3. Space-averaged electron density in the simulation of the development of a DC microdischarge, for different time steps and different treatments of the electron energy source term. Time steps larger than 10^{-10} s were impossible using an explicit energy source term evaluation. The simulated discharge configuration is shown in Fig. 2.

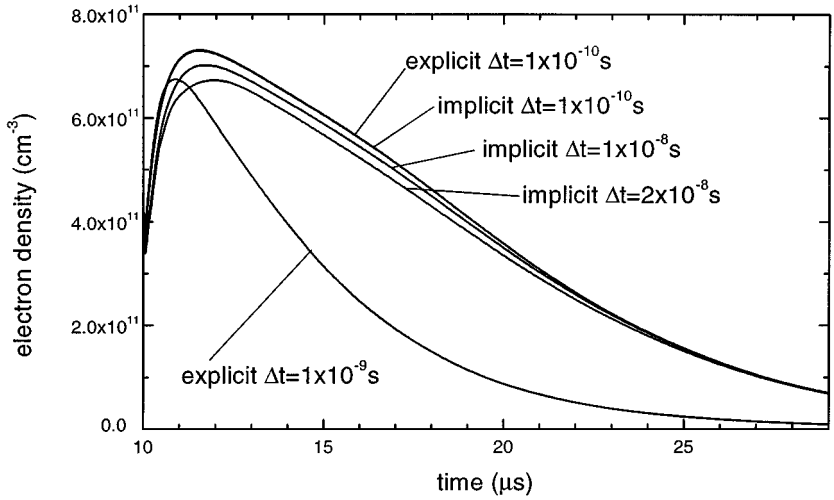

FIG. 4. Space-averaged electron density in the simulation of the afterglow of a microdischarge, for different time steps and different treatments of the electron energy source term. The simulated discharge configuration is shown in Fig. 2.

behavior of the plasma becomes dominated by ambipolar diffusion. Initially the plasma density rises, due to a sudden absence of drift losses while production is still present; then it slowly decreases. Explicit evaluation of the electron energy source term was possible up to $\Delta t = 10^{-9}$ s, but led to large inaccuracies for $\Delta t > 10^{-10}$ s. Once again implicit evaluation gave good results for $\Delta t = 10^{-8}$ s. The implicit correction of the electron heating part of the energy source term turned out to be essential for these afterglow conditions.

When one uses the large time steps of up to $\Delta t = 10^{-8}$ s, however, the semi-implicit technique for the electric field tends to produce errors if the fluxes in Poisson's equation (25)

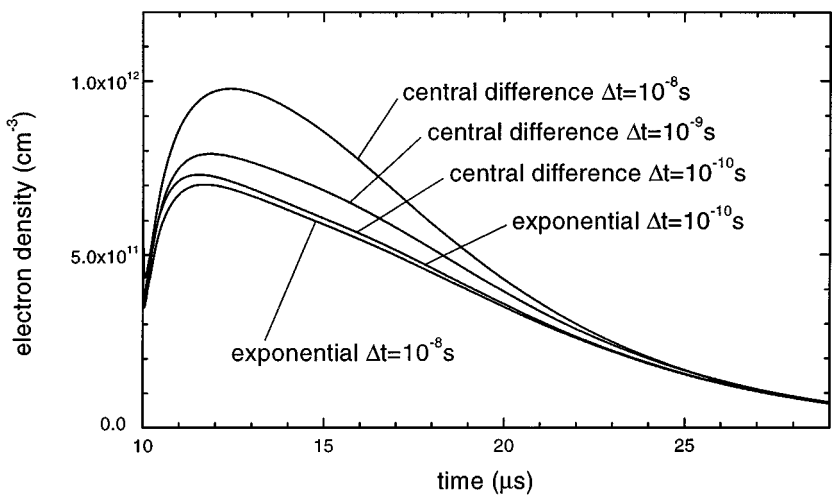

FIG. 5. Space-averaged electron density in the simulation of the afterglow of a microdischarge. The simulated discharge configuration is shown in Fig. 2. The figure compares the performances of two spatial discretization schemes for the fluxes in the semi-implicit Poisson equation (26), the central difference scheme (33), and the linearized exponential scheme (34), for different time steps. In all calculations the electron energy source term was handled implicitly.

TABLE I
Comparison between Test Results of Different Time Integration Schemes

Treatment of electric field	Treatment of electron energy source term	Typical maximum time step	Typical CPU time ratio
Explicit	Explicit	10^{-11} s, Eq. (17)	1
Implicit	Explicit	10^{-10} s	1.5×10^{-1}
Implicit	Implicit	10^{-8} s	2.0×10^{-3}

are spatially discretized according to the central difference method (32). We found that the problem can be avoided by applying the linearized exponential scheme (33) instead. As an example, Fig. 5 compares both spatial discretization schemes for the afterglow simulation, where the effect is most apparent. In all calculations the same uniform Cartesian grid was used. The grid size was appropriate for the exponential scheme; that is, further grid refinement hardly changed the results obtained with this scheme. The central difference scheme obviously requires a finer grid. We did not see the effect in steady state calculations: both discretization methods led to virtually the same steady state results, even for very large time steps.

The test results are summarized in Table I. Since the test problems cover a wide range of numerical conditions, similar results can be expected for discharge simulations in general, e.g., for RF discharge modeling.

CONCLUSIONS

If the coupling between charged particle transport and space charge field is treated implicitly or semi-implicitly, the time step in numerical fluid models for gas discharges becomes restricted by the explicit evaluation of the source term in the balance equation for electron energy. In this work we have presented an implicit technique for the energy source term, which overcomes these restrictions. For test calculations on microdischarges this implicit treatment made it possible to increase the time step by two orders of magnitude, resulting in a speedup of the calculation by almost the same factor. Since the test problems cover a wide range of numerical conditions, generalization of these results seems possible.

In addition we have shown that the semi-implicit method for the electric field can lead to large inaccuracies if a central difference scheme is used for the spatial discretization of the particle fluxes in Poisson's equation. These numerical errors can be greatly reduced by applying a linearized exponential scheme instead.

ACKNOWLEDGMENTS

This work was supported by the Philips Research Laboratories in Eindhoven, The Netherlands. The authors thank W. J. Goedheer of the FOM Institute for Plasma Physics "Rijnhuizen" in Nieuwegein, The Netherlands, for fruitful discussions.

REFERENCES

1. R. Veerasingam, R. B. Campbell, and R. T. McGrath, One-dimensional fluid and circuit simulation of an ac plasma display cell, *IEEE Trans. Plasma Sci.* **23**(4), 688 (1995).

2. K. C. Choi and K.-W. Whang, Numerical analysis of the microdischarge in a dc plasma display panel by 2-dimensional multifluid equations, *IEEE Trans. Plasma Sci.* **23**(3), 399 (1995).
3. C. Punset, J.-P. Boeuf, and L. C. Pitchford, Two-dimensional simulation of an alternating current matrix plasma display cell: Cross-talk and other geometric effects, *J. Appl. Phys.* **83**(4), 1884 (1998).
4. J. D. P. Passchier and W. J. Goedheer, A two-dimensional fluid model for an argon rf discharge, *J. Appl. Phys.* **74**, 3744 (1993).
5. J.-P. Boeuf and L. C. Pitchford, Two-dimensional model of a capacitively coupled rf discharge and comparisons with experiments in the Gaseous Electronics Conference reference reactor, *Phys. Rev. E* **51**(2), 1376 (1995).
6. G. J. Nienhuis, W. J. Goedheer, E. A. G. Hamers, W. G. J. H. van Sark, and J. Bezemer, A self-consistent fluid model for radio-frequency discharges in SiH_4–H_2 compared to experiments, *J. Appl. Phys.* **82**(5), 2060 (1997).
7. R. Morrow, Properties of streamers and streamer channels in SF6, *Phys. Rev. A* **31**, 1778 (1987).
8. S. K. Dhali and P. F. Williams, Two-dimensional studies of steamers in gases, *J. Appl. Phys.* **62**, 4697 (1987).
9. N. Yu. Babaeva and G. V. Naidis, Simulation of positive streamers in air in weak uniform electric fields, *Phys. Lett. A* **215**, 187 (1996).
10. M. S. Barnes, T. J. Colter, and M. E. Elta, Large-signal time-domain modeling of low-pressure rf glow discharges, *J. Appl. Phys.* **61**, 81 (1986).
11. J.-P. Boeuf, Numerical model of rf glow discharges, *Phys. Rev. A* **36**(6), 2782 (1987).
12. A. D. Richards, B. E. Thompson, and H. H. Sawin, Continuum modeling of argon radio frequency glow discharges, *Appl. Phys. Lett.* **50**(9), 492 (1987).
13. P. J. Roache, *Computational Fluid Dynamics* (Hermosa, Albuquerque NM, 1976).
14. K. W. Morton and D. F. Mayers, *Numerical Solution of Partial Differential Equations* (Cambridge Univ. Press, Cambridge, UK, 1994).
15. T. E. Nitschke and D. B. Graves, A comparison of particle in cell and fluid model simulations of low-pressure radio frequency discharges, *J. Appl. Phys.* **76**, 5646 (1994).
16. J.-P. Boeuf and L. C. Pitchford, *SIGLO-RF* (Kinema Research, Monument, CO, 1995).
17. P. L. G. Ventzek, T. J. Sommerer, R. J. Hoekstra, and M. J. Kushner, Two-dimensional hybrid model of inductively coupled plasma sources for etching, *Appl. Phys. Lett.* **63**, 605 (1993).
18. P. L. G. Ventzek, R. J. Hoekstra, and M. J. Kushner, Two-dimensional modeling of high plasma density inductively coupled sources for materials processing, *J. Vac. Sci. Technol. B* **12**, 461 (1994).
19. G. Lapenta, F. Iinoya, and J. U. Brackbill, Particle-in-cell simulation of glow discharges in complex geometries, *IEEE Trans. Plasma Sci.* **23**(4), 769 (1995).
20. D. L. Sharfetter and H. K. Gummel, Large-signal analysis of a silicon Read diode oscillator, *IEEE Trans. Electron Devices ED* **16**, 64 (1969).